한국광물학회지 제 16 권 제 1 호 (2003)
J. Miner. Soc. Korea, 16, 1-17 (2003)

# Mode of Occurrences and Depositional Conditions of Arsenopyrite from the Yeonhwa 1 Mine, Korea

## 연화 제1광산에서의 유비철석의 산상과 배태 조건

Young Up Lee (이영엽)* · Jae Il Chung (정재일)*

*Department of Earth & Environmental Sciences, College of Natural Sciences, Chonbuk National University, Chonju 561-756, Korea, E-mail: yulee@moak.chonbuk.ac.kr)
(전북대학교 자연대학 과학기술학부 지구환경과학과)

**ABSTRACT** : The chemical composition of the arsenopyrite Ib adjoining "triple mutual contact" arsenopyrite + pyrite + hexagonal pyrrhotite may serve as a useful geothermometer in Stage II. In this study it corresponds to temperature $\underline{T} = 330℃$ and $\underline{f}(S_2) = 10^{-9.5}$ atm. And the pyrite-hexagonal pyrrhotite buffer curve indicates the probable range of the two variables; $\underline{T} = 315 \sim 345℃$, and $\underline{f}(S_2) = 10^{-10.5} \sim 10^{-9}$ atm. The present antimony-bearing arsenopyrite (arsenopyrite Ic) is characterized by relatively high content of antimony, ranging from 4.95 to 8.91 percent Sb by weight and excess of iron and deficiency of anions are evident. Such a high antimonian arsenopyrite has never been known within single grain. But being the high content of antimony as in the arsenopyrite Ic, it does not serve as a geothermometer.

The results of microprobe analyses for four pairs of asenopyrite and sphalerite in Stage III indicate the temperature range from 310 to 340℃, and sulphur fugacity range from $10^{-10} \sim 10^{-9}$ atm. These values seem to correspond with those inferred from the Fe-As-S system.

**Key words** : *asenopyrite, Fe-As-S system, geothermometer, sulphur fugacity, microprobe analysis*

요약 : 유비철석 + 황철석 + 육방정계 자류철석으로 구성되는 "삼종동시접촉"을 수반하는 유비철석의 화학조성은 광화작용의 II단계에서 유용한 지온계를 제공한다. 연구에 따르면 이 지온계는 황분압 $f(S_2) = 10^{-9.5}$ 기압하에서, 지온 T = 330℃에서 형성된 것으로 밝혀졌다. 황철석 -육방정계 자류철석 완충곡선에서는 이 두 변수가 T = 315~345℃와 $f(S_2) = 10^{-10.5} \sim 10^{-9}$ 기압에 해당됨을 보여 준다. 이 지역에서 산출되는 안티모니를 포함하는 자류철석(Ic)는 무게 퍼센트가 4.95~8.91에 달하는 상대적인 높은 값을 보이며, 철은 과다한 반면 양이온은 결핍되는 현상을 보인다. 자류철석에서 이러한 높은 안티모니 함량은 단일 입자내에서는 처음 알려진 것이다. 이러한 높은 안티모니 함량이 자류철석 Ic를 지온계로서 작용할 수 없게 만들었다.

광화작용 III단계에서의 4쌍의 자류철석과 섬아연석의 전자현미분석 결과는 T = 310~340℃와 f(S2) = $10^{-10} \sim 10^{-9}$ atm을 보이며, 이 값은 Fe-As-S 계에서 추정된 값과 일치한다.

주요어 : 유비철석, Fe-As-S 계, 지온계, 황분압, 전자현미분석

## Introduction

Arsenopyrite, a sulpharsenide of iron (FeAsS) is familiar mineral, being distributed widely in nature and occurs in varying amounts in many metallic deposits of different genesis. The ideal formula of arsenopyrite is FeAsS, however, natural arsenopyrites usually contain small or trace amounts of nickel and cobalt which substitute for iron, and those of antimony and bismuth for arsenic. In spite of its common occurrence, the mineral has not been received the careful examination, and its crystal structure has been believed to have orthorhombic symmetry on the basis of $AX_2$ type marcasite structure for a long time (e.g., de Jong, 1926; Buerger, 1936, 1939).

Recently, Morimoto and Clark (1961) have shown that arsenic and sulphur in natural arsenopyrites can be mutually substituted to the limits of $FeAs_{0.9}S_{1.1}$ and $FeAs_{1.1}S_{0.9}$. From the results of study by means of single crystal X-ray diffraction method, they concluded that the increase of the content of arsenic leads to transformation from the space group $\underline{P}\bar{1}$ with triclinic symmetry to $\underline{P}2/\underline{c}$ with approximately monoclinic symmetry, to the unit cell approaching an orthorhombic symmetry. They also noted that changes in the position of the 131 reflection of arsenopyrites are a sensitive indicator of difference in arsenopyrite composition. The 131 reflection on the X-ray powder-diffraction pattern of arsenopyrite has sufficiently strong intensity and separates well from most extraneous materials, and since it appears at a relatively big $2\theta$ -region ($FeK_\alpha$: $2\theta = 72.6 \sim 73.1^\circ$), the $\underline{d}$-spacing may be measured precisely.

Clark (1960c) determined detailed phase relationships in the condensed Fe-As-S system between 400 and 750℃ and also investigated the effects of pressure up to 2,070 bars. Moreover, recent experimental study by Kretschmar and Scott (1976) has shown that the composition of arsenopyrite is very sensitive to sulphur fugacity, but if sulphur fugacity is buffered with sulphide assemblages, such as pyrite + hexagonal pyrrhotite and bismuthinite + native bismuth (Bi melt), the composition (As/S atomic ratio or atomic percent As) in arsenopyrite ($FeAs_{1\pm x}S_{1\pm x'}$ $0 \leqq x \leqq 0.1$) is mainly a function of the formation temperatures.

This study is made to presume temperature and pressure condition applied at formation of ore deposit using the chemical composition of the arsenopyrite. It may serve as a useful geothermometer adjoining arsenopyrite + pyrite + hexagonal pyrrhotite.

## Location and Geologic Settings

The Yeonhwa 1 mine lies about 5 km north of Seogpo station on the Ryeongdong Line of the Korean National Railway, and the mine Province, approximately at lat. 37°04 N and long. 129°02 E (Fig. 1). In the mine area, the basement rocks of Precambrian granite gneisses - "Taebaegsan Gneiss Complex" (Lee and Kim, 1984) and the overlying Cambro-Ordovician sedimentary rocks of the Joseon Supergroup are exposed extensively. The results of K/Ar radiometric dating on three members of the gneiss complex given by Yun and Silberman (1979) are as follows ; Dongjeom gneiss : 1,744±52 Ma for muscovite, pegmatite in Dongjeom gneiss : 1,754±53 Ma for muscovite, and Hongjesa granite : 730±22 Ma for biotite. This indicates that at least two phases of Precambrian intrusive and/or metamorphic events took place in the district.

The Cambro-Ordovician sediments belonging to Duwibong (platform) sequence have been divided into the following nine formations in ascending order (Cheong, 1969) ; the Jangsan Quartzite and the Myobong Slate; the Poongchon and the Hwajeol Formation ; the Dongjeom Quartzite, the Dumudong and the Magdong Formation ; and Jigunsan Slate and Duwibong Limestone. The boundary of Cambrian and Ordovician has been defined at the base of the Dongjeom Quartzite for convenience, though the biostratigraphic boundary lies at the upper horizon of the Hwajeol Formation (Kobayashi, 1953). Stocks of dykes of lamprophyre (K/Ar

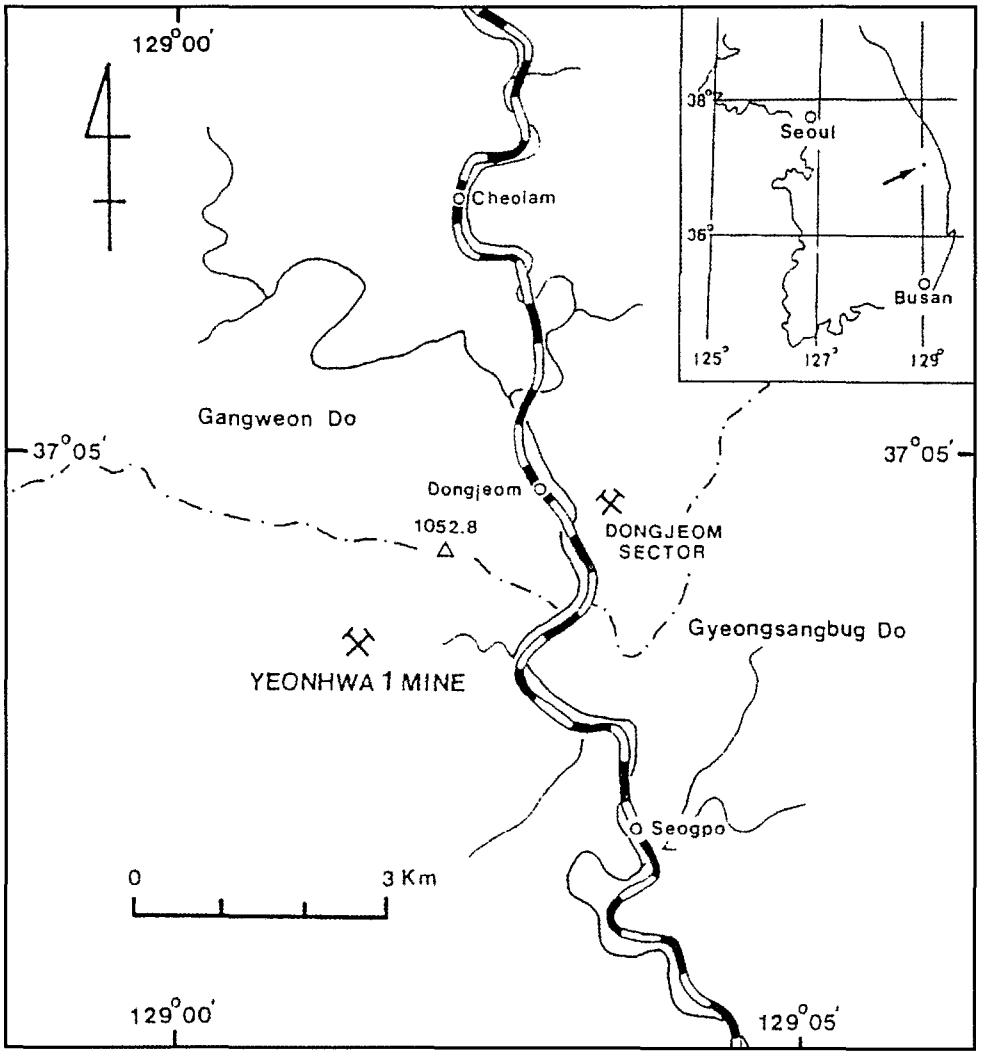


**Fig. 1.** Map showing the location of the Yeonhwa 1 Mine district.

age : 213±4 Ma on muscovite ; Yun and Silberman, 1979) have intruded into the above basement rocks and the sedimentary rocks of the Samcheog Group. Dykes of quartz-monzonite porphyry and diabase of unknown age also crop out in some places.

Structurally, the Yeonhwa 1 mine area occupies the eastern segment of the southern limb of Hambaeg syncline, whose axis trending approximately EW~NW and plunging westwards. The structure of strata on the surface in the mine area is fairly steep ; they strike NE and dip between 40° and 60° NW in general, however, in the underground dips become gentle, from 25° to 30° NW. In some places, the strata have been overturned due to local disturbance of faultings. Minor foldings and warpings are developed locally. The dominant faults in the mine area include (1) steep reverse fault of EW strike with a steep dip of about 60° in north of the mine workings, that places the Pungchon Limestones over the Hwajeol Formation, (2) steep reverse fault trending NS~N30°E, and (3) steep reverse fault striking N20~30°W with dips of 45°~85°W-SW.

## Occurrence

In the zinc-lead (-silver) ores from the Yeonhwa 1 mine, the arsenopyrite is widespread and relatively abundant. As for the features of metallic mineraizations in calcic Fe, Cu, Zn-Pb, W and Mo skarn deposits in Japan and Korea, Miyazawa (1976) has stated that the ore deposits have three stages in time evolutionary trend; Stage I: oxide stage, Stage II: sulphide stage (1), and Stage III: suphide stage (2). The arsenopyrite in the mine may be divided broadly into two species on the basis of chronological order during the stage of metallic mineralization; (1) early arsenopyrite formed Stage II (arsenopyrite I) and (2) late arsenopyrite formed Stage III (arsenopyrite II).

The arsenopyrite I usually representing the earliest mineral in Stage II, may be also classified into the following three types according to the difference in chemical properties, the assembled minerals, and in the textural relationships; the arsenopyrites Ia, Ib and Ic.

The arsenopyrite Ia is "ordinary" arsenopyrite and occurs as grains euhedral to anhedral in shape, closely associated with sphalerite, pyrrhotite (both hexagonal and monoclinic phases), and occasionally with pyrite, galena and marcasite. The size and shape of the grains are quite variable, from 20 $\mu$m to 1 mm across, and they frequently show euhedral rhomb, about 100 $\mu$m across. Lamellar twinning may be observed on some occasions. Among grains of the arsenopyrite Ia, those adjoining "triple mutual contact" arsenopyrite + pyrite + hexagonal pyrrhotite (Fig. 2(1)) are designated as the arsenopyrite Ib for convenience in the present paper.

It has already been pointed out that arsenopyrite is refractory mineral, which is "strong" against the retrograde alteration, however, as shown in Fig. 2(2), replacement of arsenopyrite by pyrrhotite may be recognized on some occasions. Also, in rare cases, pyrite or pyrrhotite may occur as veinlets along the fractures of arsenopyrite.

The arsenopyrite Ic, on the other hand, is the antimony-bearing variety (antimonian arsenopyrite) formed in Stage II, closely associated with bismuthinite and native bismuth (Fig. 3). It was found in pyrrhotite-rich ore from the orebody on - 360 m adit level. Especially, the reflectance of the arsenopyrite Ic seems higher than those of others and the isotropy of it is somewhat stronger.

The arsenopyrite II may be classified into the following two types; the arsenopyrites IIa and IId. The IIa is "ordinary" arsenopyrite, which also represents the earliest mineral in Stage III, and is closely associated with pyrite, monoclinic pyrrhotite, sphalerite and carbonates (mostly rhodochrosite) and in rare cases with galena, stannite, chalcopyrite and marcasite. It is euhedral to subhedral in form, and the grain size is quite variable from less than 10 $\mu$m to 1 mm across, but the grains 100 $\mu$m across are most common. In some euhedral rhombs of arsenopyrite, optical zoning may be visible, and replacement by chalcopyrite may be observed.

The arsenopyrite IId occurs in the carbonate and/or quartz sulphide veins, and is considered to have been formed in Stage III. These veins occur near the orebody on the -540 m adit level. The ore Specimen has been subjected to a close examination, a narrow vein about 10 cm in thickness has the symmetrical structure, in which central part is occupied by white or pinkish white part, and both outer sides consist mainly of sulphide. This arsenopyrite IId is closely associated with sphalerite, pyrite, galena and wolframite. In some parts of the polished (thin-) sections, the arsenopyrite seems to occur as the cement filling the interstices of the aggregates of lath-shaped wolframite, together with other sulphides. The arsenopyrite is coarse-grained, ranging from 100 $\mu$m to more than 1 mm across.

## Chemical Composition

As far as the arsenopyrite Ia, Ib, IIa and IId are concerned, since the qualitative microprobe analyses by spectrometer scans detected Fe, As and S alone, the other elements such as Ni, Co,

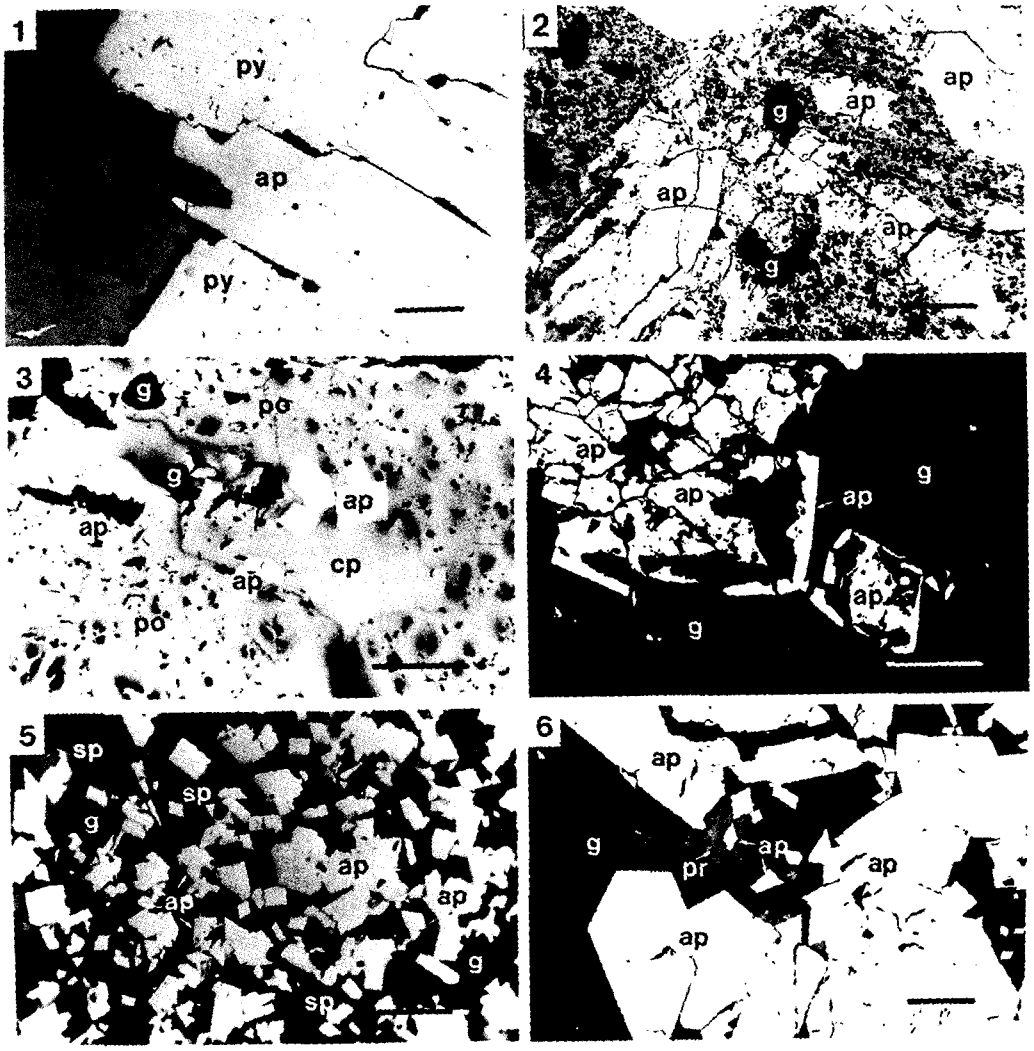


**Fig. 2.** Photomicrographs of the polished sections (one polar), showing the mode of occrrence of arsemopyrite. Bar scale indicates 100 $\mu$m in length. Abbreviation: ap = arsenopyrite. po = pyrrhotite. py = pyrite. cp = chalcopyrite. g = galena. pr= pyrargyrite. sp = sphalerite.

Sb and Bi, which may enter into arsenopyrite structure were below the detection limits of microprobe. On some occasions, natural arsenopyrites contain minor or trace amounts of antimony and bismuth, which seem generally missing (Ramdohr, 1980). The present antimony-bearing arsenopyrite (arsenopyrite Ic) is characterized by relatively high content of antimony, ranging from 4.95 to 8.91 percent Sb by weight and excess of iron and deficiency of anions are evident. Such a high antimonian arsenopyrite has never been known in within single grains and at the study of it, the X-ray diffraction method seems desirable. In the case of the arsenopyrite Ic, in addition to Fe, As and S, Sb was detected, but Ni, Co and Bi were not detected.

*Arsenopyrites Ia, Ib and IIa*

Based on quantitative microprobe analyses (Table 1), the arsenopyrites Ia, Ib and IIa are characterized by the excess of sulphur and

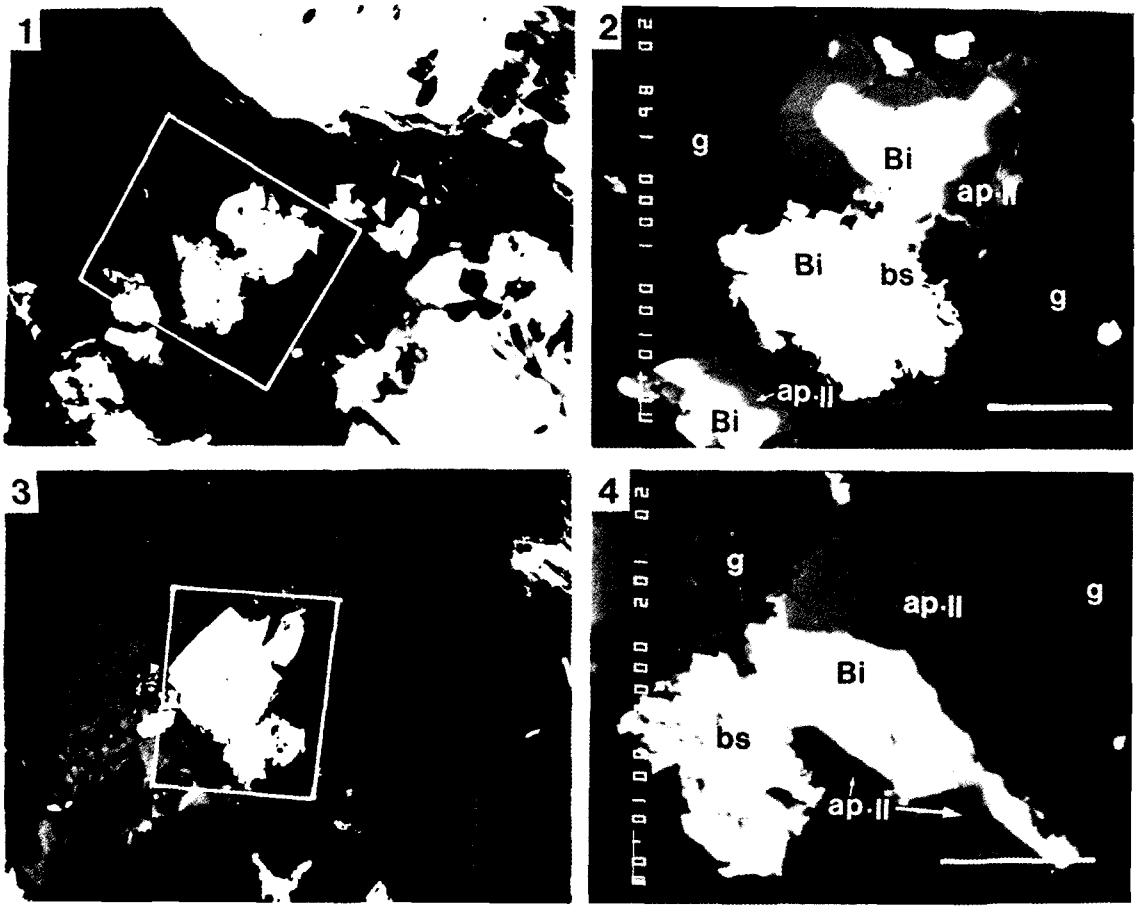


**Fig. 3.** Photomicrographs and the back-scattered electron (compositional) images, showing the mode of occurrence of arsenopyrite Ic. (1) and (3) : Photomicrographs in the reflected light (one polar). (2) : Back-scattered electron (compositional) image of the area of rectangular marked in (1), counter clockwise rotation. (4) : Back-scattered electron (compositional) image of the area of rectangular marked in (3), clockwise rotation. Bar scale of (2) indicates 30 $\mu$m and that of (4) 40 $\mu$m in length. Abbreviation: ap = arsenopyrite. bi = native bithmuth. bs = bithmuthinite. g = galena.

deficiency of arsenic deviating slightly from stoichiometric composition FeAsS. Careful microprobe analyses were made for ten spots in the optically and chemically homogeneous area near the "triple mutual contact" of arsenopyrite + pyrite + hexagonal pyrrhotite (Fig. 1(1)) and the results are listed in Table 2. The arithmetic mean value of atomic percent As for ten analyses is $30.56 \pm 0.59$.

*Arsenopyrite Ic (antimonian arsenopyrite)*

The photomicrographs of the polished sections and the back-scattered electron images of the area of rectangle showing the mode of occurrence of the arsenopyrite Ic are reproduced in Fig. 3. Also, X-ray scanning images corresponding to the Fig. 3(4) by characteristic X-rays of Ask$\alpha$, SbL$\alpha$, FeK$\alpha$, BiM$\alpha$ and SK$\alpha$ are given in Fig. 4. These figures qualitatively show that marked concentration of antimony is taken place within the arsenopyrite Ic.

The selected electron microprobe analyses for ten spots in the discrete four grain are listed in Table 3, from which it is noted that the present arsenopyrite Ic is characterized by the relatively

**Table 1.** Selected electron-microprobe analyses of arsenopyrite

| Po. | Gr. | Weight percent | | | | Atomic percent | | | 100As/S |
|---|---|---|---|---|---|---|---|---|---|
| | | Fe | As | S | Total | Fe | As | S | |
| 1 | A | 34.90 | 44.75 | 20.85 | 100.50 | 33.37 | 31.90 | 34.73 | 91.85 |
| 2 | B | 34.76 | 44.75 | 20.85 | 100.36 | 33.28 | 31.94 | 34.78 | 91.83 |
| 3 | C | 34.57 | 45.01 | 20.62 | 100.20 | 33.23 | 32.25 | 34.52 | 93.42 |
| 4 | D | 34.93 | 43.60 | 20.96 | 99.49 | 33.60 | 31.27 | 35.13 | 89.01 |
| 5 | E | 34.45 | 43.37 | 20.50 | 98.32 | 33.61 | 31.54 | 34.84 | 90.53 |
| 6 | F | 35.38 | 43.97 | 20.54 | 99.89 | 34.04 | 31.54 | 34.43 | 91.61 |
| 7 | G | 34.66 | 44.45 | 20.56 | 99.67 | 33.45 | 31.98 | 34.57 | 92.51 |
| 8 | H | 34.82 | 44.24 | 20.50 | 99.56 | 33.64 | 31.86 | 34.50 | 92.35 |
| 9 | I | 34.46 | 43.25 | 21.16 | 98.87 | 33.27 | 31.13 | 35.59 | 87.46 |
| 10 | J | 34.29 | 42.77 | 21.14 | 98.20 | 33.29 | 30.95 | 35.75 | 86.57 |
| 11 | K | 35.47 | 43.94 | 20.64 | 100.05 | 34.05 | 31.44 | 34.51 | 91.10 |
| 12 | L | 35.80 | 43.14 | 21.39 | 100.33 | 34.02 | 30.56 | 35.41 | 86.30 |
| 13 | M | 34.87 | 43.52 | 20.44 | 98.83 | 33.88 | 31.52 | 34.60 | 91.10 |
| 14 | N | 34.29 | 43.75 | 20.34 | 98.38 | 33.51 | 31.87 | 34.62 | 92.06 |
| 15 | O | 34.95 | 44.20 | 20.47 | 99.62 | 33.75 | 31.82 | 34.43 | 92.42 |
| 16 | P | 36.44 | 43.19 | 21.26 | 100.89 | 34.48 | 30.47 | 35.05 | 86.93 |
| 17 | Q | 35.01 | 42.99 | 22.49 | 100.49 | 32.95 | 30.17 | 36.88 | 81.81 |
| 18 | R | 34.49 | 42.99 | 22.50 | 99.98 | 32.62 | 30.31 | 37.07 | 81.76 |
| 19 | S | 34.53 | 42.82 | 22.54 | 99.89 | 32.66 | 30.19 | 37.14 | 81.29 |

Po. : Point number. Gr. : Grain number.

**Table 2.** Selected electron-microprobe analyses of arsenopyrite with "triple mutual contact"

| Po. | Gr. | Weight percent | | | | Atomic percent | | | 100As/S |
|---|---|---|---|---|---|---|---|---|---|
| | | Fe | As | S | Total | Fe | As | S | |
| 1 | A | 36.12 | 42.66 | 21.67 | 100.45 | 34.18 | 30.09 | 35.72 | 84.24 |
| 2 | B | 35.93 | 43.49 | 21.25 | 100.67 | 34.10 | 30.77 | 35.13 | 87.59 |
| 3 | C | 35.97 | 43.72 | 21.40 | 101.09 | 33.98 | 30.79 | 35.22 | 87.42 |
| 4 | D | 36.07 | 43.07 | 21.46 | 100.60 | 34.17 | 30.42 | 35.41 | 85.91 |
| 5 | E | 36.37 | 42.66 | 21.77 | 100.80 | 34.28 | 29.97 | 35.75 | 83.83 |
| 6 | F | 35.92 | 43.47 | 21.27 | 100.66 | 34.09 | 30.75 | 35.16 | 87.46 |
| 7 | G | 35.91 | 43.53 | 21.41 | 100.85 | 33.99 | 30.71 | 35.30 | 87.00 |
| 8 | H | 35.74 | 43.61 | 21.44 | 100.79 | 33.84 | 30.71 | 35.30 | 87.00 |
| 9 | I | 35.85 | 43.51 | 21.36 | 100.70 | 33.97 | 30.75 | 35.28 | 87.16 |
| 0 | J | 35.87 | 43.52 | 21.48 | 100.87 | 33.93 | 30.68 | 35.39 | 86.69 |

Po. : Point number. Gr. : Grain number

high content of antimony, ranging from 4.95 to 8.91 weight percent Sb and marked excess of iron and deficiency of sulphur from the stoichiometric composition and the compositional heterogeneity within the single grains. In order to clarify the mutual relationships of these atoms of metal, semimetal and sulphur, these chemical data obtained by microprobe analyzer were processed in the following several manners for the assumed chemical formula Fe(As + Sb)S, indicating substitution of Sb for As.

Fig. 5 shows the relation of Sb versus As, from which it is seen that, the content of As exhibits approximate reverse relationship to that of Sb content, suggesting As → Sb substitution. Also, compositional relationships of Fe, As and Sb are plotted into the enlarged parallerogram in the triangle diagram Fe-As-Sb (Fig. 6). Although not so clear, the iron content tends to increasing with increase antimony content (Fig. 7). This is

**Table 3.** Selected electron-microprobe analyses of Sb-bearing arsenopyrite

| Po. | Gr. | Weight percent | | | | | Atomic percent | | | | 100As * /S |
|---|---|---|---|---|---|---|---|---|---|---|---|
| | | Fe | As | Sb | S | Total | Fe | As | Sb | S | |
| 1 | A | 35.45 | 39.13 | 4.95 | 19.96 | 99.49 | 34.87 | 28.69 | 2.23 | 34.20 | 90.41 |
| 2 | A | 35.68 | 37.90 | 6.12 | 19.04 | 98.74 | 35.71 | 28.28 | 2.81 | 33.20 | 93.64 |
| 3 | A | 35.15 | 37.07 | 8.91 | 18.79 | 99.92 | 35.29 | 27.74 | 4.10 | 32.86 | 96.90 |
| 4 | B | 35.11 | 38.65 | 7.76 | 18.69 | 100.21 | 35.10 | 28.80 | 3.56 | 32.55 | 99.42 |
| 5 | B | 34.85 | 42.77 | 5.28 | 17.98 | 100.88 | 34.68 | 31.73 | 2.41 | 31.17 | 109.53 |
| 6 | C | 35.08 | 40.12 | 5.95 | 18.07 | 99.22 | 35.36 | 30.15 | 2.75 | 31.73 | 103.69 |
| 7 | C | 34.90 | 37.27 | 7.85 | 18.49 | 98.51 | 35.43 | 28.21 | 3.66 | 32.70 | 97.46 |
| 8 | D | 34.65 | 41.24 | 5.34 | 17.79 | 99.02 | 35.06 | 31.11 | 2.48 | 31.35 | 107.11 |

Po. : Point number. Gr. : Grain number, As * represents As + Sb

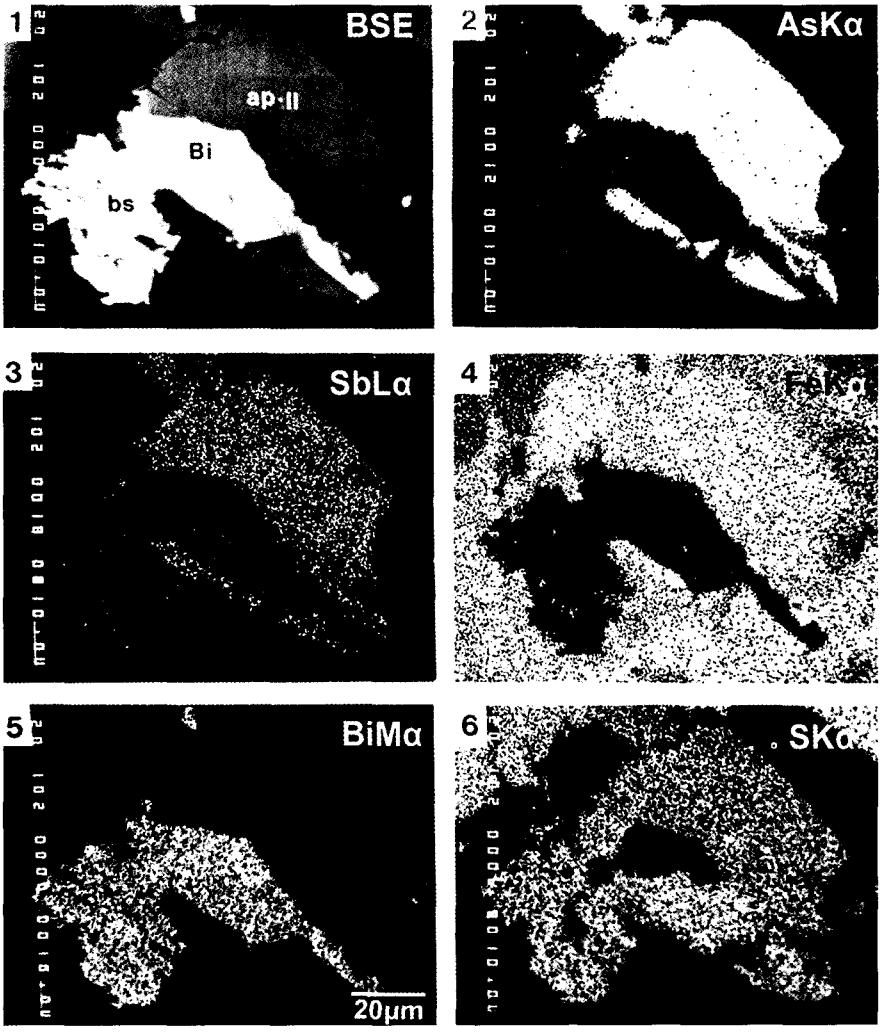


**Fig. 4.** Back-scattered electron (compositional) image and corresponding X-ray images, showing the textural features of arsenopyrite Ic. The area corresponds to the area of rectangle in the photomicrograph as shown in Fig. 3(4). (1) : Back-scattered electron (compositional) image. (2)~(6) : Characteristic X-ray images.

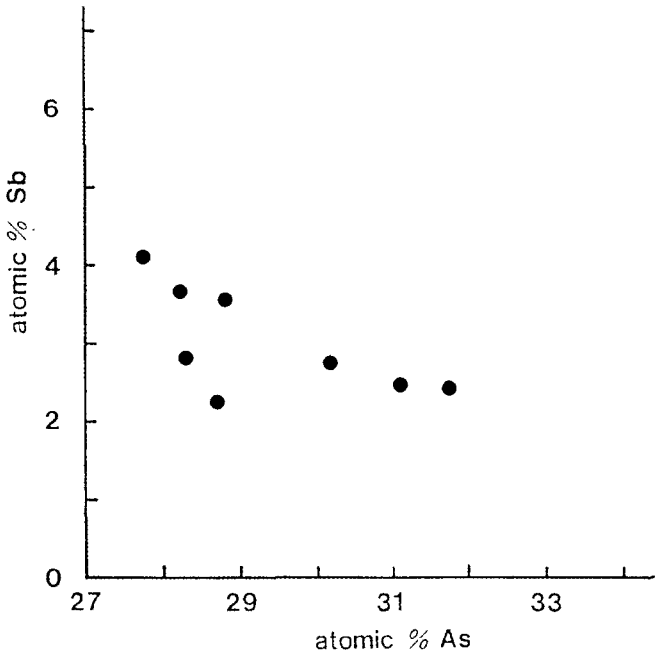


**Fig. 5.** Variation diagram showing the relation of Sb versus As in arsenopyrite Ic (atomic percent).

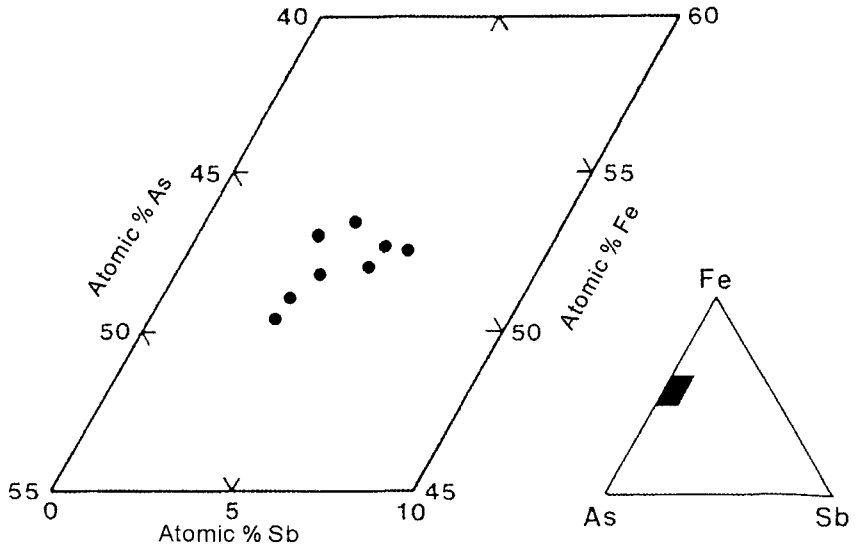


**Fig. 6.** Enlarged parallelogram in the triangle diagram of the system Fe-As-Sb, showing the chemical composition of arsenopyrite Ic.

also suggested from Fig. 8 showing the reverse relation of iron content versus arsenic content. Finally, the analytical results are summarized by Fig. 9 of triangle diagram Fe-(As + Sb)-S.

*Arsenopyrite IId*

Quantitative analyses of the arsenopyrite IId have been made for only four spots near the

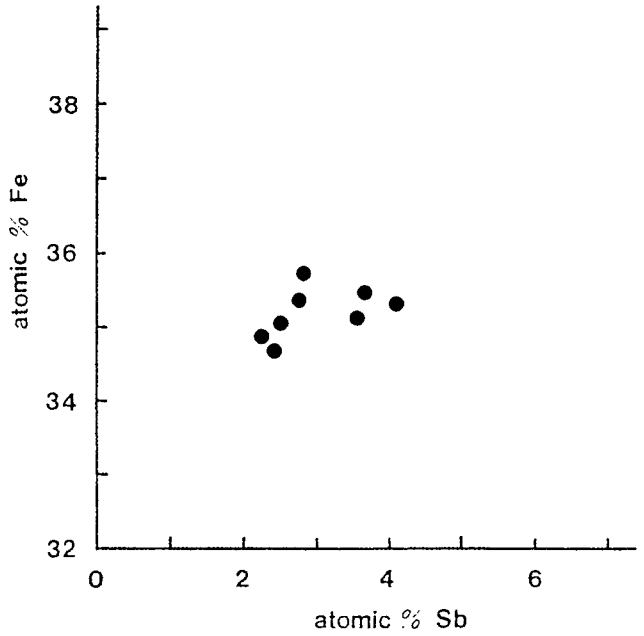


**Fig. 7.** Variation diagram showing the relation of Fe versus Sb in arsenopyrite Ic (atomic percent).

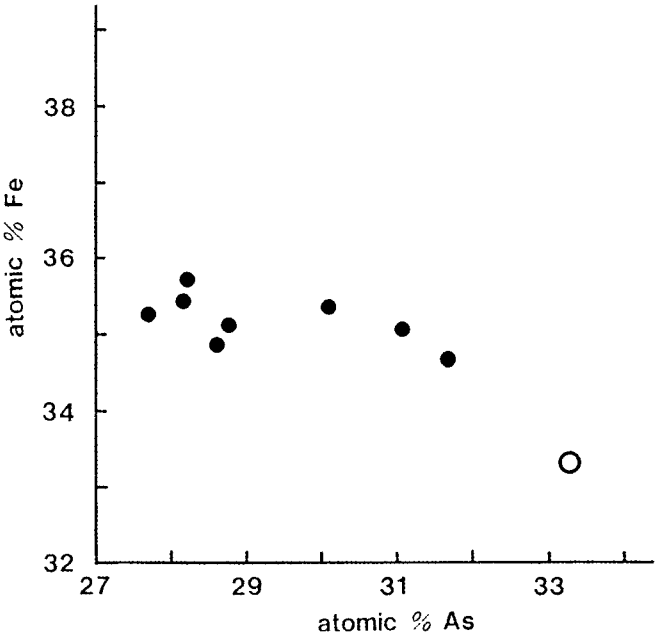


**Fig. 8.** Variation diagram showing the relation of Fe versus As in arsenopyrite Ic (atomic percent). Full small circles represent the compositions from the Yeonwha 1 mine. Open circle shows the composition calculaated from the ideal formula FeAsS.

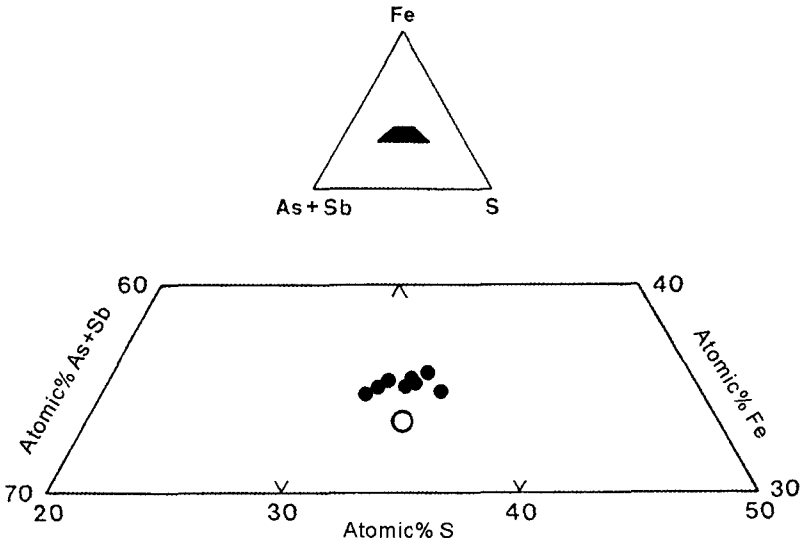


**Fig. 9.** Enlarged parallelogram in the triangle diagram of the system Fe-(As + Sb) - S, showing the chemical composition of arsenopyrite Ic. Full small circles represent the compositions from the Yeonwha 1 mine. Open circle shows the composition calculated from the ideal formula FeAsS.

contact with sphalerite. The results are listed in Table 1, showing the deficiency of arsenic and excess of sulphur deviating considerably from the stoichiometric composition; namely, the content of arsenic ranges from 30.17~30.47 mole percent As. These compositional data for the arsenopyrite IId and those of the co-existing sphalerite will be utilized as "arsenopyrite-sphalerite geothermometer".

The enlarged parallerogram in the triangle diagram Fe-(As + Sb)-S as shown in Fig. 10 summarizes the chemical compositions of all arsenopyrites from the Yeonhwa 1 mine. Also, Fig. 11 represents the histogrammatic representation between frequency and atomic percent As for major groups of the arsenopyrites.

## Composition of Arsenopyrite as a Indicator of Temperature and Sulphur Fugacity

*General statements*

The composition of arsenopyrite, the atomic ratio As/S or atomic percent As, is very sensitive to sulphur fugacity (activity), $\underline{f}(S_2)$. The experimental study on the phase relations of the system Fe-As-S by Kretschmar and Scott (1976) shows, however, that the compositions of arsenopyrites ($FeAs_{1\pm x}S_{1\pm x}$, $0 \leqq x \leqq 0.1$) is mainly a function of temperatures, only when the mineral comes from sulphur-buffer assemblages, such as arsenopyrite + pyrite + hexagonal pyrrhotite and arsenopyrite + native bismuth + bismuthinite. Arsenopyrite having the most refractory nature is unlikely to change its composition in response to the subsequent variation of the conditions, and it is a useful tool for deciphering the physicochemical environments during its crystallization.

Morimoto and Clark (1961) has suggested that the atomic ratio As/S of arsenopyrite decreases with increasing confining pressure (S-rich trend). However, Kretschmar and Scott (1976) have given a pseudo-binary $\underline{T}$-$\underline{X}$ diagram along the pyrite ($FeS_2$)-lollingite ($FeAs_2$) join, based upon their experimental results for the condensed Fe-As-S system. In low pressure region, they have ignored the pressure effects on the phase

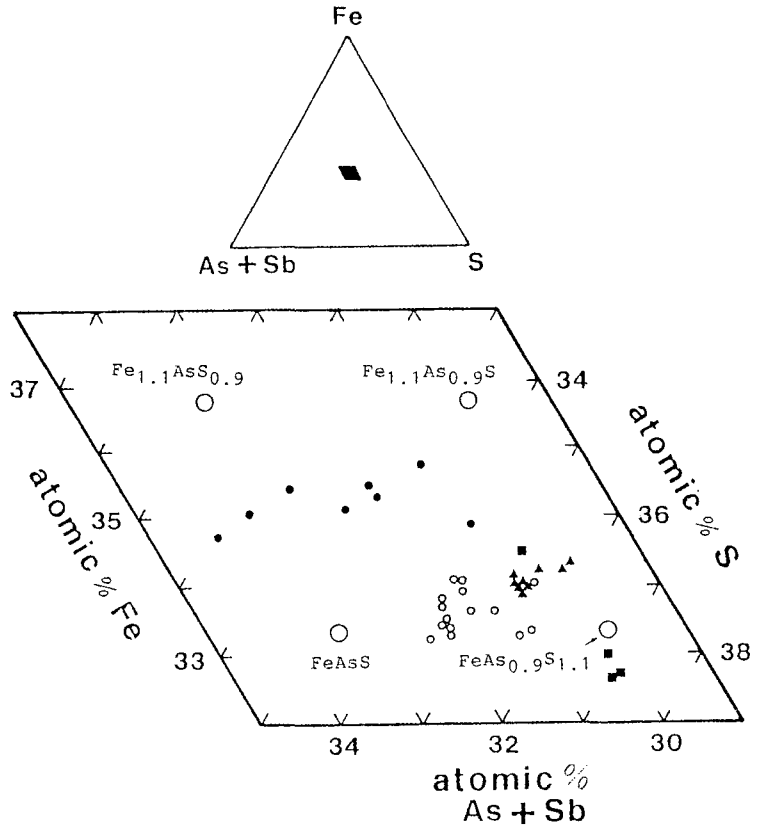


**Fig. 10.** Enlarged parallelogram in the triangle diagram of the system Fe-(As + Sb) - S, showing the chemical composition of arsenopyrite Ic. Open circles : drdinary arsenopyrite. Full circles : Sb bearing arsenopyrite. Full triangles : "triple mutual contact" arsenopyrite. Full squares : arsenopyrite contacted with sphalerite.

relations, and stressed its role as a geothermometer, provided that minor element content does not exceed 1 weight percent. These authors have observed significant variation for the atomic ratio As/S of arsenopyrite grains in the same specimen, even though the specimen has sulphur-buffer assemblage, and they attribute this to the local variation of $f(S_2)$ during its crystallization.

Among the Yeonhwa 1 arsenopyrites with two generations during mineralization, only arsenopyrite Ib having "triple mutual contact" arsenopyrite + pyrite + hexagonal pyrrhotite is permissible for geothermometer.

*Experimental procedures*

The arsenopyrite Ib having "triple mutual contact" was searched for polished sections under the ore microscope. In this case also, distinction of hexagonal pyrrhotite from the monoclinic modification was performed by the Bitter's colloidal suspension method using magnetite colloids. Analytical points within arsenopyrite grains were selected adjacent to the "triple point" as near as possible, where the area is homogeneous in both optcally and compositionally, and then careful microprobe analysis was carried out. Special attentions were paid for the analysis of arsenic, using the standards of

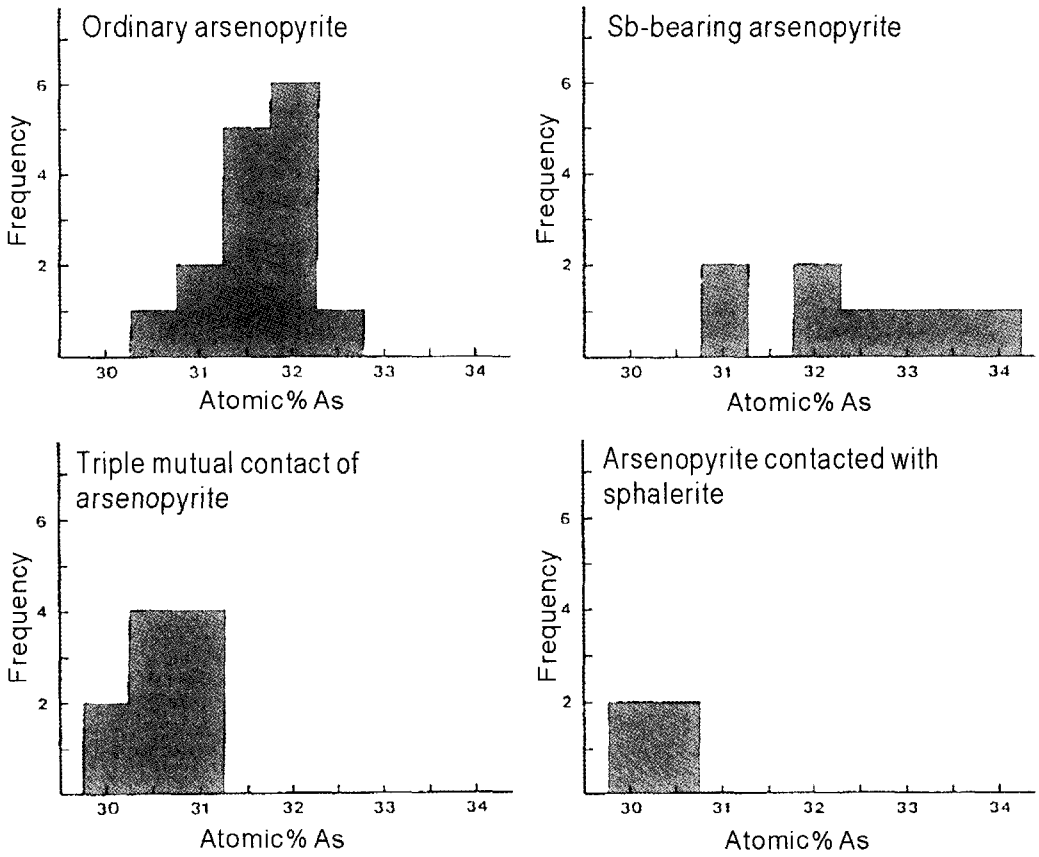


**Fig. 11.** Histograms showing the frequency of the mole percent FeS in arsenopyrite.

extra-pure single crystals GaAs and InAs.

*Results and discussion*

The results of microprobe analyses were already given in Table 2, indicating that the asenopyrite Ib is S-excess and As-deficient species, ranging 30.09 to 30.79 atomic percent As, with arithmetic mean 30.57 atomic percent As. The bismuthinite-Bi (melt) buffer curve lies within the stability field of arsenopyrite in the temperature-sulphur fugacity diagram of the Fe-As-S system, accordingly the intersection of this curve with isopleths of arsenopyrite indicates the invariant point, showing the unique values of both temperature and sulphur fugacity (Kretschmar and Scott, 1976; Choi, S.G. et al., 1985). As seen in Fig. 12, which was given by Kretschmar and Scott (1976), this corresponds to temperature $\underline{T} = 330℃$ and $\underline{f}(S_2) = 10^{-9.5}$ atm. Shaded area along the pyrite-hexagonal pyrrhotite buffer curve indicates the probable range of the two variables; $\underline{T} = 315 \sim 345℃$, and $\underline{f}(S_2) = 10^{-10.5} \sim 10^{-9}$ atm.

## Arsenopyrite-Sphalerite Geothermometery

*General statements*

In ore specimens containing wolframite, the assemblage arsenopyrite + sphalerite + pyrite is observed. Also these three minerals show mutual contact, suggesting that they were crystallized simultaneously. If these three minerals represent the equilibrium assemblage, the chemical composi-

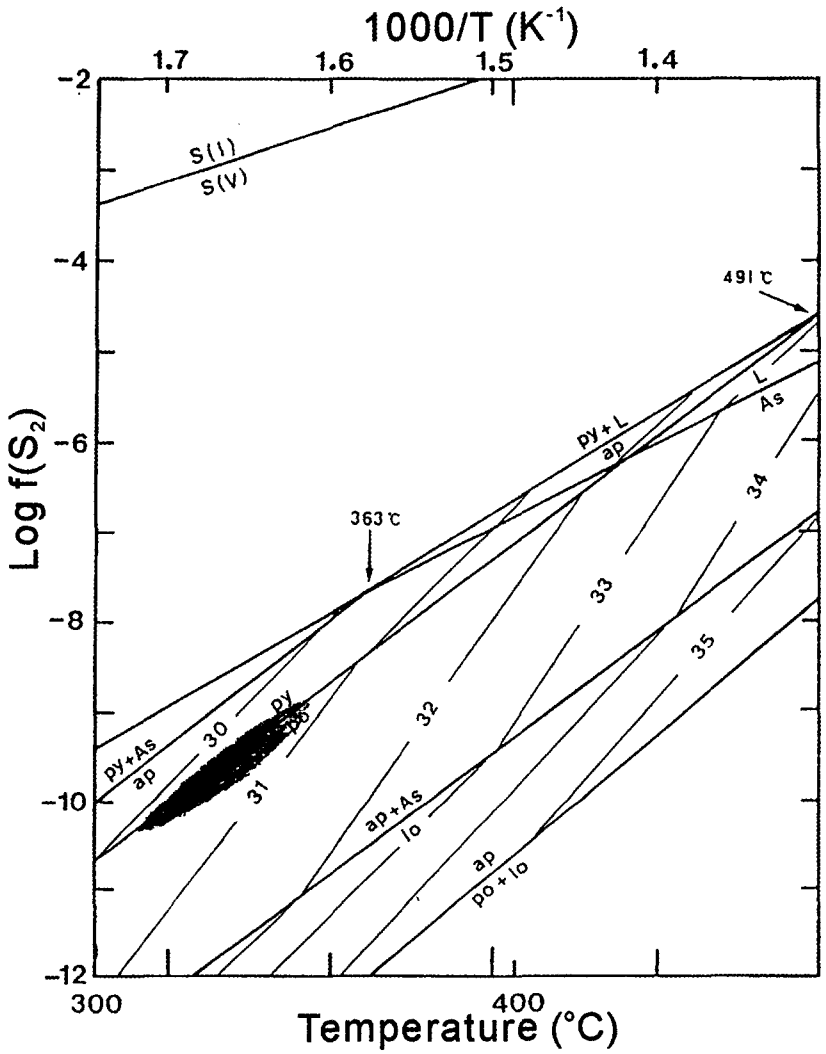


**Fig. 12.** Activity of $S_2$-temperature projection of the stability field of arsenopyrite, contoured in atomic percent arsenic (after Kretschmar and Scott, 1976). Abbreviation: ap = arsenopyrite. po = pyrrhotite. py = pyrite.

tions of arsenopyrite and sphalerite may serve as geothermometer. As indicated by Fig. 13, pyrite-pyrrhotite buffer curve lies within the stability field of arsenopyrite, and the stability field of arsenopyrite + pyrite is constrained to a narrow belt. When the diagram showing the compoaition in terms of mole fraction FeS of sphalerite, $\underline{X}^{sp}$FeS in equilibrium with pyrrhotite and pyrite as a function of fugacity of sulphur, $\underline{f}(S_2)$ and temperature, $\underline{T}$ given by Scott and Barnes(1971) is superimposed upon Fig. 13 given Kretschmar and Scott(1976), the intersection of isopleth of As (Atomic percent As) in Arsenopyrite with isopleth in sphalerite ($\underline{X}^{sp}$FeS) represents the unique values of $\underline{f}(S_2)$ and temperature.

*Analytical procedures*

"Triple mutual contact" of arsenopyrite + sphalerite + pyrite was searched under the ore microscope. Anlytical points were selected as near as the triple point. Preliminary microprobe

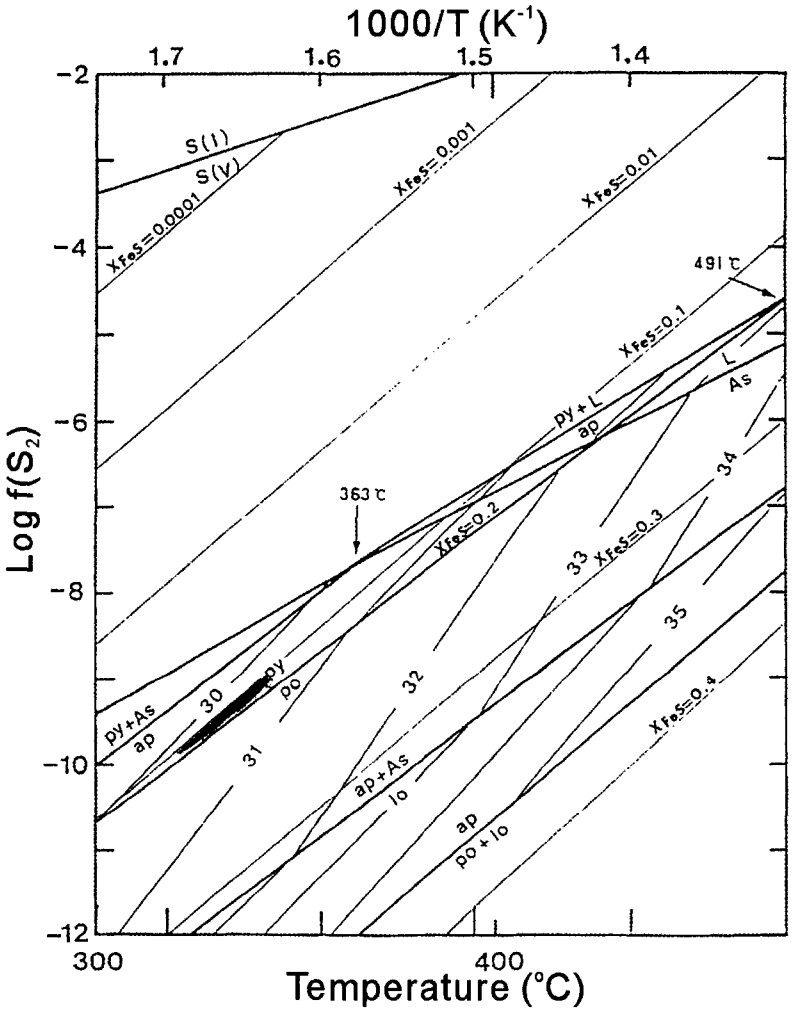


**Fig. 13.** Activity of $S_2$-temperature projection of the stability field of arsenopyrite contoured in atomic percent arsenic and sphalerite contoured in atomic proportion on the basis of 1 sulphur. $X_{FeS}$ represents mole fraction of FeS in sphalerite (after Kretschmar and Scott, 1976). Abbreviation: ap = arsenopyrite. po = pyrrhotite. py = pyrite.

analyses for sphalerite were made to confirm the compositional range of sphalerite. As a result, it was confirmed that the average composition yields the formula $(Fe_{0.16}Zn_{0.82}Cu_{0.01}Cd_{0.00})\Sigma_{0.99}S_{1.00}$, which lies within the stability field of pyrite in Fig. 13.

*Results and discussion*

The results of microprobe analyses for four pairs of asenopyrite and sphalerite are listed in Table 4 and 5. Also the results are shown as shaded area in Fig. 13, which indicate the temperature range from 340 to 310℃, averaging 330℃, and sulphur fugacity range from $10^{-9}$~$10^{-10}$ atm, averaging $10^{-10}$ atm. The tungsten mineralization with subsequent deposition of arsenopyrite + sphalerite + pyrite assemblage is considered to represent the initial phase of Stage III and the temperature and sulphur fugacity values

**Table 4.** Selected electron-microprobe analyses of arsenopyrite associated with sphalerite

| Point | Grain | Weight percent | | | | Atomic proportion on the basis of total = 3.00 | | |
|---|---|---|---|---|---|---|---|---|
| | | Fe | As | S | Total | Fe | As | S |
| 1 | A | 36.44 | 43.19 | 21.26 | 100.89 | 1.035 | 0.914 | 1.051 |
| 2 | B | 35.01 | 42.99 | 22.49 | 100.49 | 0.989 | 0.914 | 1.051 |
| 3 | C | 34.49 | 42.99 | 22.50 | 99.98 | 0.979 | 0.909 | 1.112 |
| 4 | D | 34.53 | 42.82 | 22.54 | 99.89 | 0.980 | 0.906 | 1.114 |

**Table 5.** Selected electron-microprobe analyses of sphalerite associated with arsenopyrite

| Point | Grain | Weight percent | | | | | |
|---|---|---|---|---|---|---|---|
| | | Zn | Fe | Cu | Cd | S | Total |
| 1 | A | 56.84 | 8.90 | 0.15 | 0.25 | 33.05 | 99.19 |
| 2 | B | 55.51 | 9.73 | 0.05 | 0.33 | 33.23 | 98.85 |
| 3 | C | 54.81 | 9.11 | 2.71 | 0.13 | 33.76 | 100.52 |
| 4 | D | 56.61 | 8.73 | 0.07 | 0.22 | 33.43 | 99.06 |
| Point | Grain | Atomic proportion on the basis of S = 1 | | | | | |
| | | Zn | Fe | Cu | Cd | Total | |
| 1 | A | 0.843 | 0.155 | 0.002 | 0.002 | 1.002 | |
| 2 | B | 0.819 | 0.168 | 0.001 | 0.003 | 0.991 | |
| 3 | C | 0.155 | 0.796 | 0.040 | 0.001 | 0.993 | |
| 4 | D | 0.831 | 0.150 | 0.001 | 0.002 | 0.983 | |

seem appropriate to the consideration from the above Fe-As-S system.

## Conclusions

Among the Yeonhwa 1 arsenopyrites with two generations during mineralization, only arsenopyrite Ib having "triple mutual contact" arsenopyrite + pyrite + hexagonal pyrrhotite is permissible for geothermometer. The chemical composition of the arsenopyrite Ib may serve as a useful geothermometer in Stage II, provided that the assemblage is in equilibrium. The bismuthinite-Bi (melt) buffer curve lies within the stability field of arsenopyrite in the temperature-sulphur fugacity diagram of the Fe-As-S system, accordingly the intersection of this curve with isopleths of arsenopyrite indicates the invariant point, showing the unique values of both temperature and sulphur fugacity. In this study it corresponds to temperature $\underline{T}$ = 330℃ and $\underline{f}(S_2) = 10^{-9.5}$ atm. And the pyrite-hexagonal pyrrhotite buffer curve indicates the probable range of the two variables; $\underline{T}$ = 315~345℃, and $\underline{f}(S_2) = 10^{-10.5} \sim 10^{-9}$ atm.

On some occasions, natural arsenopyrites contain minor or trace amounts of antimony and bismuth. But the present antimony-bearing arsenopyrite (arsenopyrite Ic) is characterized by relatively high content of antimony, ranging from 4.95 to 8.91 percent Sb by weight and excess of iron and deficiency of anions are evident. Such a high antimonian arsenopyrite has never been known in within single grains and at the study of it, the X-ray diffraction method seems desirable. In the arsenopyrite Ic, however, unfortunately it does not serve as a geothermometer, because of its high content of antimony. The results of microprobe analyses for four pairs of asenopyrite and sphalerite Stage III indicate the temperature range from 340 to 310 ℃, and sulphur fugacity range from $10^{-10} \sim 10^{-9}$ atm. These values seem to concord with those inferred from the Fe-As-S system. It means that in the zinc-lead (- silver) ores formation analysis, the arsenopyrite geothermometery and

geobarometery can be also used.

## References


Buerger, M.J. (1936) The symmetry and crystal structure of the minerals of the arsenopyrite group. Z. Krist., v. 95, p. 136-137.

Buerger, M.J. (1939) The crystal structure of gudmundite(FeSbS) and its bearing on the existence field of arsenopyrite structural type. Z. Krist., v. 101. 290-316.

Choi, S.G., Chung J.I. and Imai, N. (1985) Compositional variation of arsenopyrite in polymetallic ores from the Ulsan mine, Republic of Korea, and their application to a geothermometer (abst. in Japanese). Coll. Abst. Autumn Joint Meet., Miner. Soc. Japan, Soc. Mining Geol. Japan and Japanese Assoc. Miner. Petrolog. Eco. Geol., C-35, p.134.

Cheong, C.H. (1969) Stratigraphy and paleontology of the Samcheog Coalfield, Gangwon-do, Korea (1)(in Korean with Englixh abst.). J. Geol. Soc. Korea, v. 5, p. 13-56.

Clark, L.A. (1960c) The Fe-As-S aystem. Variations of arsenopyrite composition as a function of T and P. Carnegie Inst. Wash. Year B., v.59, p. 127-130.

de Jong, W.F. (1926) Bepaling van de absolute as lengten van markasiet en daarmee isomorfe mineralen. Physica, Nederland Tijds. Naturk, v. 6, p. 325-332.

Lee, S.M. and Kim, H.S. (1984) Metamorphic Studies on the so-called Yulri and Wonnam Groups in the Mt. Taebaeg Area(in Korean with Englixh abst.). J. Geol. Soc. Korea, v. 20, p. 195-214.

Kobayashi, T. (1953) The Cambro-Ordovician Formations and Faunas of Chosen, pt. 4, Geology of South Korea with special reference to the Limestone Plateau of Gangwon-do(Kogendo). Imp. Univ. Tokyo Fac. Sci. J., Sect. 2, v. 8, pt. 4, p.145-293.

Kretschmar, U. and Scott, S.D. (1976) Phases relation involving arsenopyrite in the system Fe-As-S and their application. Canad. Miner., v. 14, p. 364-386.

Miyazawa, T. (1976) Contact-metasomatic deposits in Japan and Korea. In Studies of Contact-metasomatic deposits. A3-A149.

Morimoto, N. and Clark, L.A. (1961) Arsenopyrite crystal-chemical relations. Am. Miner., v. 46, p. 1448-1469.

Ramdohr, P. (1980) The ore minerals and their intergrowths. Pergamon Press, 2nd ed.

Scott, S.D. and Barnes, H.L. (1971) Sphalerite geothermometry and geobarometry. Econ. Geol., v. 66, p. 653-669.

Yun, S.K., and Silberman, M.L. (1979) K-Ar geochronology of igneous rocks in the Yeonhwa-Ulchin zinc-lead district and southern margin of the Taebaegsan basin, Korea. J. Geol. soc. Korea., v. 15, p. 1013-1032.


2002년 11월 4일 원고접수, 2002년 12월 9일 게재승인.